

## DISK-ACCRETION ONTO A BLACK HOLE. II. EVOLUTION OF THE HOLE\*†

KIP S. THORNE

California Institute of Technology, Pasadena, California

Received 1974 December 26

### ABSTRACT

When a black hole swallows matter and radiation from an accretion disk, its mass  $M$  and angular momentum  $J \equiv Ma$  change—i.e., the hole evolves. The details of that evolution are calculated. The accreting matter, by itself, would spin the hole up to  $a = M$  ("extreme-Kerr hole") after a modest amount of accretion ( $\Delta M/M_i \sim 1.5$ ). However, the radiation emitted by the disk and swallowed by the hole produces a counteracting torque, which prevents spin-up beyond a limiting state of  $(a/M)_{\text{lim}} \simeq 0.998$ . This limiting state corresponds to a maximum efficiency of 30 percent for the hole's conversion of accreting mass into outgoing photon energy. In § IV it is argued that realistic phenomena ignored in this calculation (magnetic fields dragged down the hole by accreting matter; heating of outer parts of disk by X-rays from inner parts; . . .) might not change significantly the values  $(a/M)_{\text{lim}} \simeq 0.998$  and (maximum efficiency)  $\simeq 0.30$ .

*Subject headings:* black holes — rotation

### I. INTRODUCTION

How do the properties of a black hole change as it accretes matter from its surroundings? This question was first raised by Bardeen (1970) in a landmark paper—a paper that persuaded astrophysicists to stop using the Schwarzschild metric to describe black holes and start using the Kerr metric.

Bardeen, motivated by work of Lynden-Bell (1969), considered accretion from a disk of gas orbiting the hole. He assumed that the disk lay in the equatorial plane of a Kerr hole, and that from the last stable circular orbit (inner edge of disk,  $r = r_{\text{ms}}^1$ ) the gas was dumped directly down the hole. Each gas particle carried into the hole a specific energy  $E^+ = (-p_t/m_0)$  and a specific angular momentum  $L^+ = p_\phi/m_0$  equal to the values for the last stable circular orbit,  $E_{\text{ms}}^+$  and  $L_{\text{ms}}^+$ . No other stress-energy was allowed to cross the horizon—or, more precisely, the effects of all other stress-energy were ignored. Consequently, the accretion of a rest mass  $\Delta M_0$  led to changes in the hole's total mass-energy  $M$  and total angular momentum  $J$  given by

$$\Delta M = E_{\text{ms}}^+ \Delta M_0, \quad \Delta J = L_{\text{ms}}^+ \Delta M_0;$$

and the evolution of the hole was described by the differential equations

$$\frac{da_*}{d \ln M} \equiv \frac{d(J/M^2)}{d \ln M} = \frac{1}{M} \frac{L_{\text{ms}}^+(a_*, M)}{E_{\text{ms}}^+(a_*)} - 2a_*, \quad (1a)$$

$$dM/dM_0 = E_{\text{ms}}^+(a_*). \quad (1b)$$

Using the explicit dependences of  $L_{\text{ms}}^+$  and  $E_{\text{ms}}^+$  on  $a_*$  and  $M$ , Bardeen integrated these differential equations to obtain the evolution laws

$$\begin{aligned} a_* &= \left(\frac{2}{3}\right)^{1/2} \frac{M_i}{M} \left[ 4 - \left(\frac{18M_i^2}{M^2} - 2\right)^{1/2} \right] && \text{for } 0 \leq a_* \leq 1, \quad 1 \leq \frac{M}{M_i} \leq 6^{1/2} \\ &\simeq 1 - 2(1 - 6^{-1/2}M/M_i)^3 && \text{for } 0 \leq (6^{1/2} - M/M_i) \ll 1, \\ a_* &= 1 && \text{for } M/M_i \geq 6^{1/2}; \end{aligned} \quad (2a)$$

$$M_0 - M_{0i} = 3M_i [\sin^{-1}(M/3M_i) - \sin^{-1}(1/3)] \quad \text{for } 1 \leq M/M_i \leq 6^{1/2},$$

$$M_0 - M_{0i} = 3M_i [\sin^{-1}(2/3)^{1/2} - \sin^{-1}(1/3)] + 3^{1/2}(M - 6^{1/2}M_i) \quad \text{for } M/M_i \geq 6^{1/2}. \quad (2b)$$

Here  $M_{0i}$  and  $M_i$  are constants of integration. They are the values of  $M_0$  (the rest mass that has gone down the hole) and  $M$  (the total mass-energy of the hole) when  $a_* = 0$  (hole nonrotating). (To describe accretion from an

\* See first footnote to preceding paper (Page and Thorne 1974).

† Supported in part by the National Science Foundation [GP-36687X].

<sup>1</sup> My notation is the same as that in Page and Thorne (1974)—cited henceforth as Paper I—and also the same as that in Novikov and Thorne (1973), with these exceptions dictated by typography limitations: (i) A dagger is used in place of a tilde ( $E^+$  in place of  $\tilde{E}$ ); (ii) for indices on orthonormal bases, parentheses are used in place of hats ( $e_{(r)}$  in place of  $\hat{e}_r$ ;  $p_{(\phi)}$  in place of  $\hat{p}_\phi$ ).

initial state with  $a_* \neq 0$ , one need only adjust the constants  $M_i$  and  $M_o$  appropriately.) The above formulae and this paper are restricted to the case of a disk which rotates in the same direction as does the hole. The extension to counterrotating disks would be straightforward.

According to Bardeen's evolution law (2), a black hole, which is initially nonrotating ( $a_* \equiv J/M^2 = 0$ ) and has initial mass  $M_i$ , gets spun up to the extreme-Kerr state ( $a_* = 1$ ) by the accretion of a rest mass  $\Delta M_o$  and total mass-energy  $\Delta M$  given by

$$\Delta M_o = 3[\sin^{-1}(2/3)^{1/2} - \sin^{-1}(1/3)]M_i = 1.8464M_i, \quad (3a)$$

$$\Delta M = (6^{1/2} - 1)M_i = 1.4495M_i. \quad (3b)$$

This spin-up to  $a_* = 1$  by the accretion of a finite amount of rest mass probably violates<sup>2</sup> the third law of black-hole mechanics—a law that was formulated recently by Bardeen, Carter, and Hawking (1973). Hence, processes ignored in Bardeen's analysis can be expected to modify the simple evolution law (2) so as to keep  $a_* < 1$  always.

The most important process ignored by Bardeen is the capture of the photons that are emitted by the accreting disk. The hole's capture cross-section is greater for photons of negative angular momentum (angular momentum opposite to that of the hole) than for photons of positive angular momentum (Godfrey 1970, as corrected by Bardeen 1973, pp. 229–236). This suggests that the captured photons will be less effective than the disk's gas in spinning up the hole—i.e., that the captured photons will lower  $da_*/d \ln M$  below the Bardeen value (eq. [1]), and will thereby prevent complete spin-up to  $a_* = 1$ .

In this paper we calculate explicitly the influence of photon capture on the evolution of the hole. The assumptions that underlie our calculation are spelled out in § II; the results are presented in § III; the sensitivity of our results to our assumptions is described in § IV; and the relevance of our results in various astrophysical contexts is discussed in § V. The details of the calculations are relegated to an Appendix.

## II. ASSUMPTIONS

Our results on black-hole evolution are based on the following assumptions:

(i)–(ix): The assumptions listed in § II of Paper I (Page and Thorne 1974).

(x) *Assumption*: The spacetime geometry outside the black hole is that of Kerr.

(xi) *Assumption*: The only stress-energy that crosses the horizon is that carried by material which falls freely inward from  $r = r_{ms}$ , and that carried by photons which are emitted from the disk's surface.

(xii) *Notation*: Consider an observer directly above the disk's surface (or directly below) at radius  $r$ . Let this observer move about the hole in an equatorial, circular geodesic orbit [approximately the mean motion of the matter, according to assumption (vi)]. Denote by  $I(\Theta, \Phi)$  the time-averaged intensity of emitted radiation as measured by this observer.<sup>3</sup> Here  $\Theta$  is polar angle on the observer's local "sky," measured downward from the observer's zenith (angle relative to  $e_{(z)}$ ); and  $\Phi$  is azimuth (angle in  $[e_{(r)}, e_{(\phi)}]$ -plane) measured with origin on the hole's outward radial direction ( $e_{(r)}$  direction). Then the locally measured energy emitted by a unit surface area of the disk per unit time into a unit solid angle about the  $(\Theta, \Phi)$  direction is

$$\frac{d(\text{energy measured by observer})}{d(\text{proper time of observer})d(\text{solid angle measured by observer})d(\text{area of disk measured by observer})} = I(\Theta, \Phi) \cos \Theta. \quad (4)$$

*Assumption*: Either the time-averaged emission is isotropic (case *a*):

$$\langle I(\Theta, \Phi) \rangle \text{ independent of } \Theta \text{ and } \Phi; \quad (5a)$$

or else it is "limb-darkened" in the manner expected for an electron-scattering atmosphere (case *b*):

$$\langle I(\Theta, \Phi) \rangle \propto 1 + 2 \cos \Theta \quad (5b)$$

(cf. § 68 of Chandrasekhar 1950).

(xiii) *Assumption*: Once a photon has been emitted by the disk, it travels freely along a null geodesic of the Kerr metric until it either goes down the hole or "escapes to infinity." No photons are recaptured by the disk.

This "no recapture" assumption is surely incorrect. Of the photons emitted from the inner regions of the disk, roughly 30 percent will actually get recaptured (Chris Cunningham, private communication). From outer regions, recapture is less important. Fortunately, the evolution of the hole is insensitive to the  $\lesssim 30$  percent errors in photon emission caused by our "no recapture" assumption. (For discussion and proof see § IV.)

One can best understand the significance of our assumptions by examining the ways in which they may break down. This is done in § IV.

<sup>2</sup> I say "probably violates" because the third law is today a conjecture rather than a proved theorem.

<sup>3</sup> Our terminology and notation for radiative transfer and for the basis vectors  $e_{(a)}$  of the orbiting observer are those of Novikov and Thorne (1973), §§ 2.6 and 5.4. See also n. 1.

## III. RESULTS

Figures 1 and 2 depict the evolution of a black hole, as calculated (see Appendix) from the assumptions of § II. Notice that the effect of the photons is to “buffer”  $a_*$  away from the extreme Kerr value of 1. If  $a_*$  is initially very close to 1 ( $0.999 \leq a_* \leq 1$ ), a small amount of accretion ( $\Delta M/M \lesssim 0.05$ ) quickly spins the hole down to a limiting state of  $a_{*lim} \simeq 0.998$ . If  $a_*$  is initially below this limiting value, accretion spins the hole up toward it. So long as  $a_*$  is less than 0.90 (region not shown in fig. 1), the photons have negligible effect, and the evolution (spin-up) follows the Bardeen law closely. But as  $a_*$  rises above 0.90, photon effects come into play, deflecting the evolution away from the Bardeen law and toward  $a_{*lim} \simeq 0.998$ .

Notice that the limiting value of  $a_*$  is not very sensitive to large (factor of 3) changes in the photon emission law: it is 0.9978 for isotropic emission (“I”; eq. [5a]) and 0.9982 for the electron-scattering emission law (“ES”; eq. [5b]). For further discussion see § IV.

We shall use the word “canonical” to describe a black hole and its accreting disk in the limiting case of  $a_* = a_{*lim} \simeq 0.998$ . Although the canonical value of  $a_*$  ( $\simeq 0.998$ ) is very near the extreme-Kerr value (1.0), the spacetime geometry of a canonical hole and the structure of its disk are significantly different from those of extreme Kerr. This is because the properties of the Kerr metric change very rapidly as one moves away from  $a_* = 1$ .

Table 1 lists the efficiencies with which various types of holes (Schwarzschild, canonical, extreme-Kerr) convert rest mass into outgoing radiation. The efficiency is defined by

$$\text{Efficiency} \equiv \left[ \frac{\text{(rate, as measured at “infinity,” at which photon energy)} \right. \\ \left. \text{(as measured at “infinity,” emerges from disk to “infinity”)} \right. \\ \left. \text{(rate, as measured at “infinity,” at which rest)} \right. \\ \left. \text{mass-energy is being deposited into disk)} \right]_{\text{time avg.}} \quad (6)$$

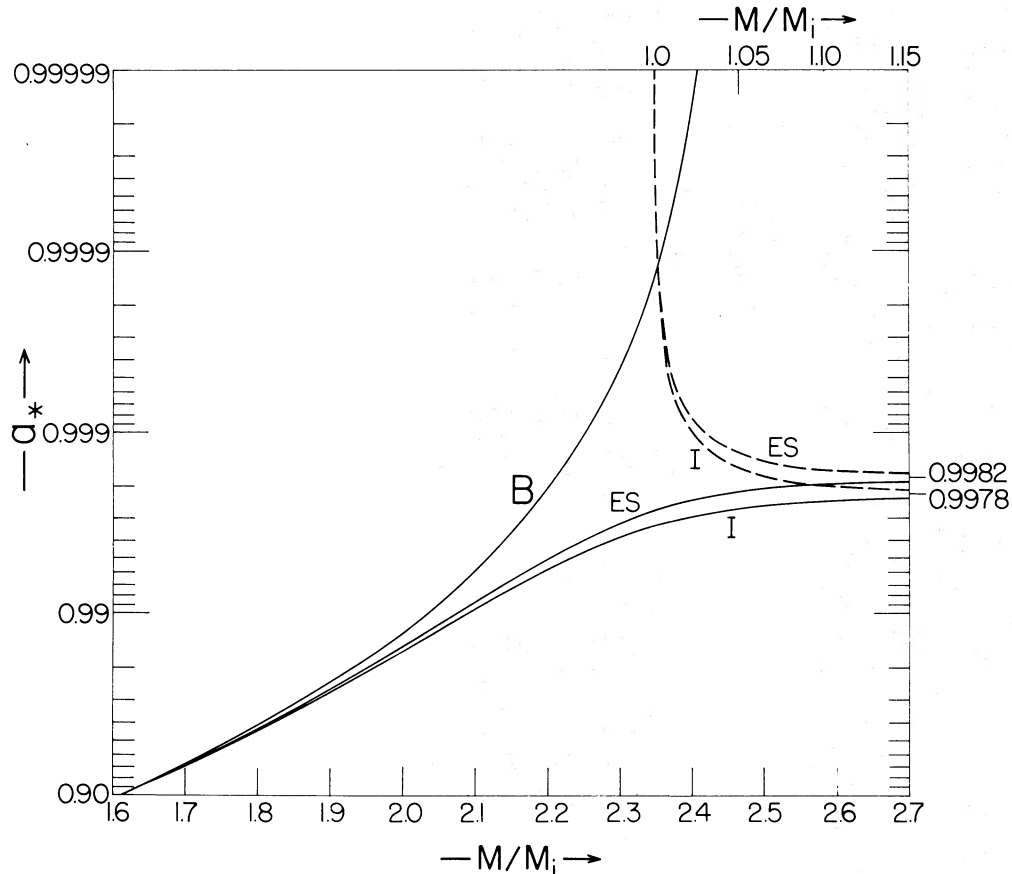


FIG. 1.—The evolution of a black hole during disk accretion: Angular momentum divided by square of mass,  $a_* \equiv J/M^2 \equiv a/M$  (dimensionless), as a function of mass  $M$  in units of  $M_i$ . For the solid curves (horizontal scale given at bottom of figure)  $M_i$  is the value of  $M$  when  $a_* = 0$ . For the dashed curves (horizontal scale given at top of figure),  $M_i$  is the value of  $M$  when  $a_* = 1$ . The solid curve  $B$  is the Bardeen evolution law (eq. [2a]; capture of photons by hole forbidden, or at least ignored). The curves  $I$  and  $ES$  are the evolution laws taking account of captured photons;  $I$  is for a disk with isotropic local photon emission (eq. [5a]);  $ES$  is for a disk with the electron-scattering emission law (eq. [5b]). The dashed curves are the predicted evolution when  $a_*$  is initially larger than 0.9978 ( $I$ ) or 0.9982 ( $ES$ ). The solid curves are for initial  $a_*$ 's less than 0.9978 ( $I$ ) or 0.9982 ( $ES$ ).

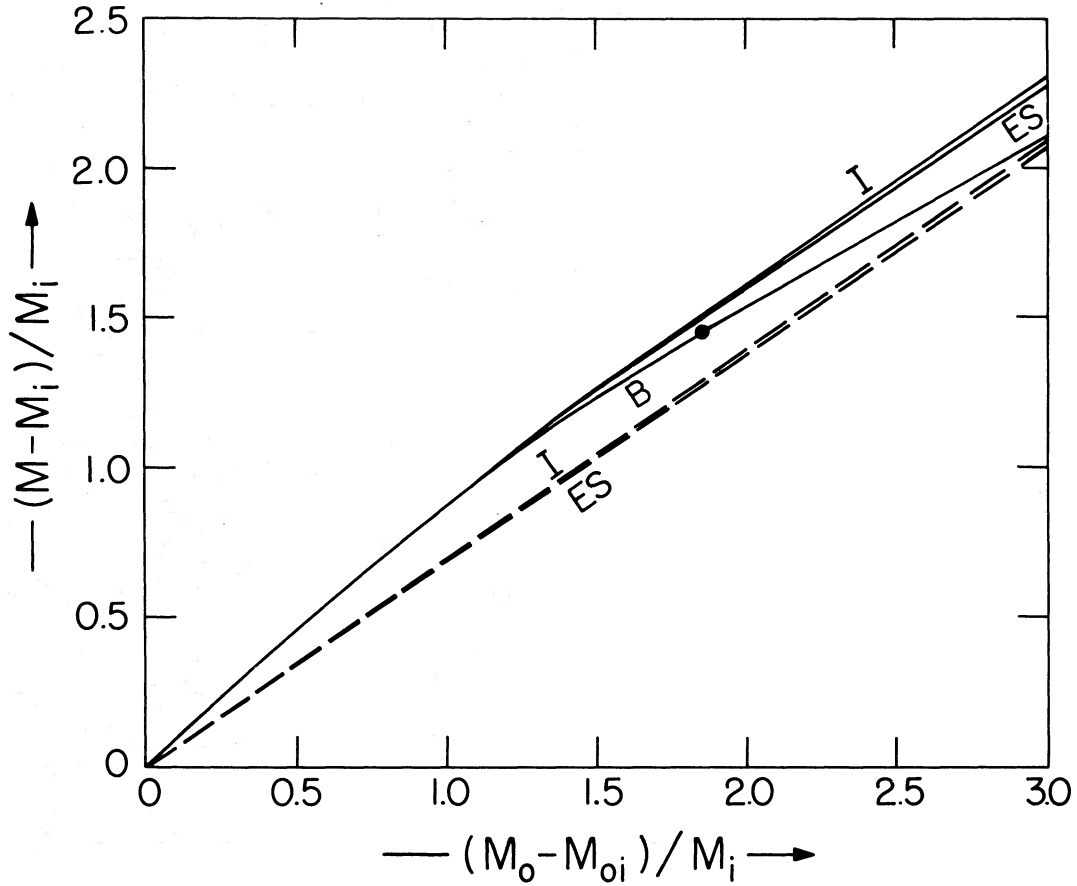


FIG. 2.—The evolution of a black hole during disk accretion: Total mass-energy (mass-energy measured by distant Keplerian orbits)  $M$  as a function of the total rest mass  $M_0$  accreted.  $M_i$  and  $M_{0i}$  are constants: the values of  $M$  and  $M_0$  when  $a_* = 0$  (solid curves), or when  $a_* = 1$  (dashed curves); cf. fig. 1. Curve B is the Bardeen evolution law (eq. [2b]). Curves I and ES take account of captured photons with an isotropic emission law (I; eq. [5a]) or an electron-scattering emission law (ES; eq. [5b]). The dashed curves correspond to initial  $a_*$ 's larger than 0.9978 (I) or 0.9982 (ES). The solid curves are for initial  $a_*$ 's smaller than 0.9978 (I) or 0.9982 (ES).

TABLE 1  
EFFICIENCY FOR CONVERTING ACCRETED MASS INTO OUTGOING RADIATION

$a_* = a/M$	Type of Hole	Efficiency, Ignoring Capture of Radiation by Hole*	Efficiency with Capture of Radiation by Hole
0. ....	Schwarzschild	0.0572	0.0570
0.9978. ....	"Canonical," with isotropic emission (eq. [5a])	0.318	0.302
0.9982. ....	"Canonical," with electron-scattering atmosphere (eq. [5b])	0.324	0.308
1.0. ....	Extreme Kerr, with isotropic emission (eq. [5a])	0.423	0.399
1.0. ....	Extreme Kerr, with electron-scattering atmosphere (eq. [5b])	0.423	0.400

\* Equal to  $1 - E_{ms}^+$ .

If all photons emitted could escape to "infinity" (no capture by hole; column [3] of table 1), then we would have

$$\text{Efficiency} = 1 - E_{ms}^{\dagger} \tag{7}$$

The capture of photons decreases the efficiency below this value, but only by a small amount (column [4]).

The most important implication of table 1 is this: in astrophysical calculations one should not use the extreme-Kerr value of 42 percent for the efficiency of conversion of rest mass to outgoing radiation. The maximum possible efficiency is more nearly 30 percent.

Figures 3 and 4 depict the time-averaged radial distribution of photon emission for disks around a canonical black hole (fig. 3) and a Schwarzschild black hole (fig. 4). Notice that for a canonical hole the locally measured flux reaches its maximum deep inside the ergosphere, where relativistic gravity is extremely important. Presumably the

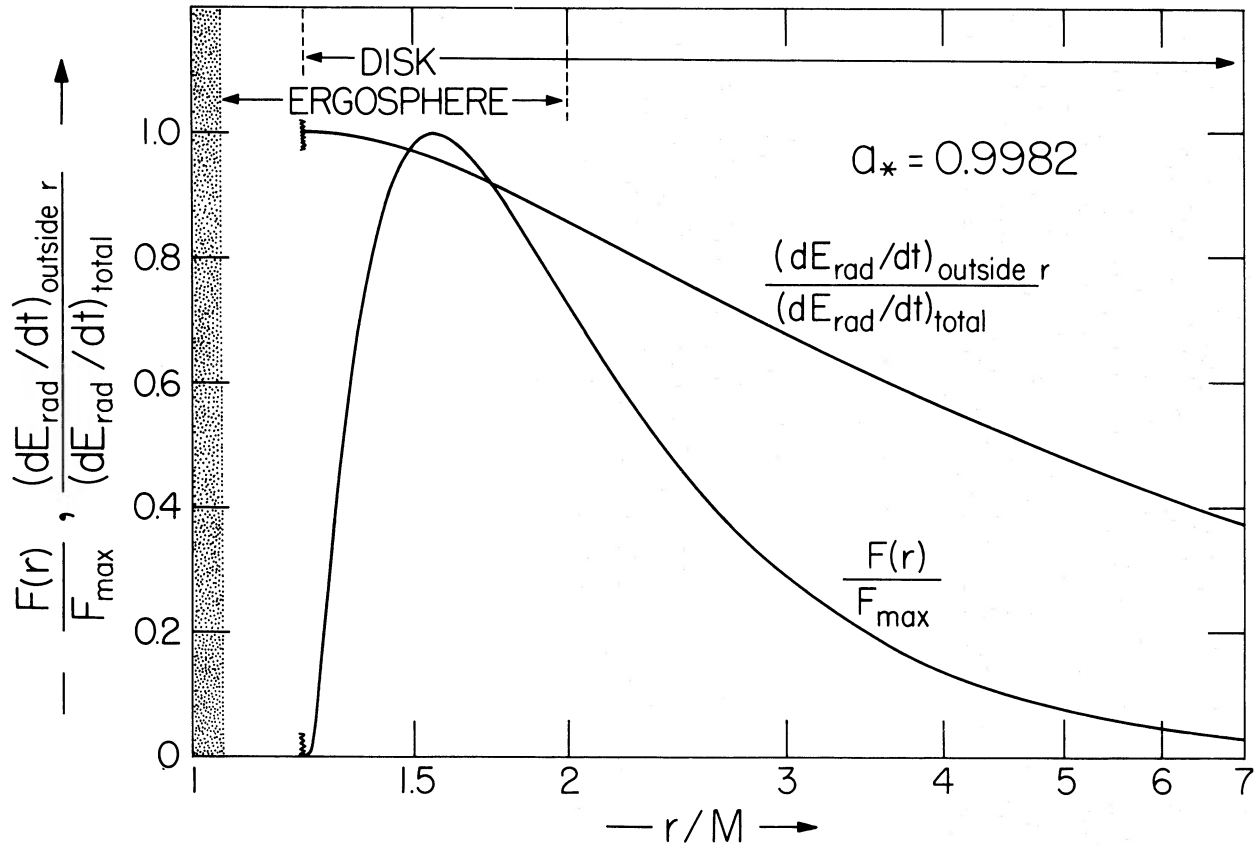


FIG. 3.—The energy radiated (time-average) by a disk around a canonical black hole ( $a_* = 0.9982$ ). The energy is depicted in two ways: *First*, in terms of the flux  $F(r)$  measured by a local observer who orbits the hole on a circular geodesic orbit:

$$F(r) \equiv \frac{d(\text{locally measured energy})}{d(\text{area of disk measured by observer})d(\text{proper time of observer})} = [\text{eqs. (11b) and (15d, n) of Paper I}].$$

If the disk were to emit as a blackbody, the orbiting observer would measure a blackbody temperature at radius  $r$  of

$$T_{bb}(r) = [F(r)/\sigma]^{1/4},$$

where  $\sigma$  is the Stefan-Boltzmann constant. The maximum value of the flux is

$$F_{\max} = 0.00498 \dot{M}_o / M^2,$$

where  $\dot{M}_o$  is the rate of accretion of rest mass (rate per unit *coordinate* time  $t$ ), and  $M$  is the mass of the hole. *Second*, the energy radiated is depicted in terms of

$$\frac{(dE_{rad}/dt)_{\text{outside } r}}{(dE_{rad}/dt)_{\text{total}}} \equiv \frac{(\text{"energy-at-infinity," } E = -p_t, \text{ emitted per unit coordinate time by that part of disk which is outside of radius } r)}{(\text{"energy-at-infinity" emitted per unit coordinate time by the entire disk})}$$

(eqs. [A2] and [A3] of Appendix). In this quantity no attention is paid to the ultimate fate of the photons: they are counted equally whether they go down the hole or escape to infinity.

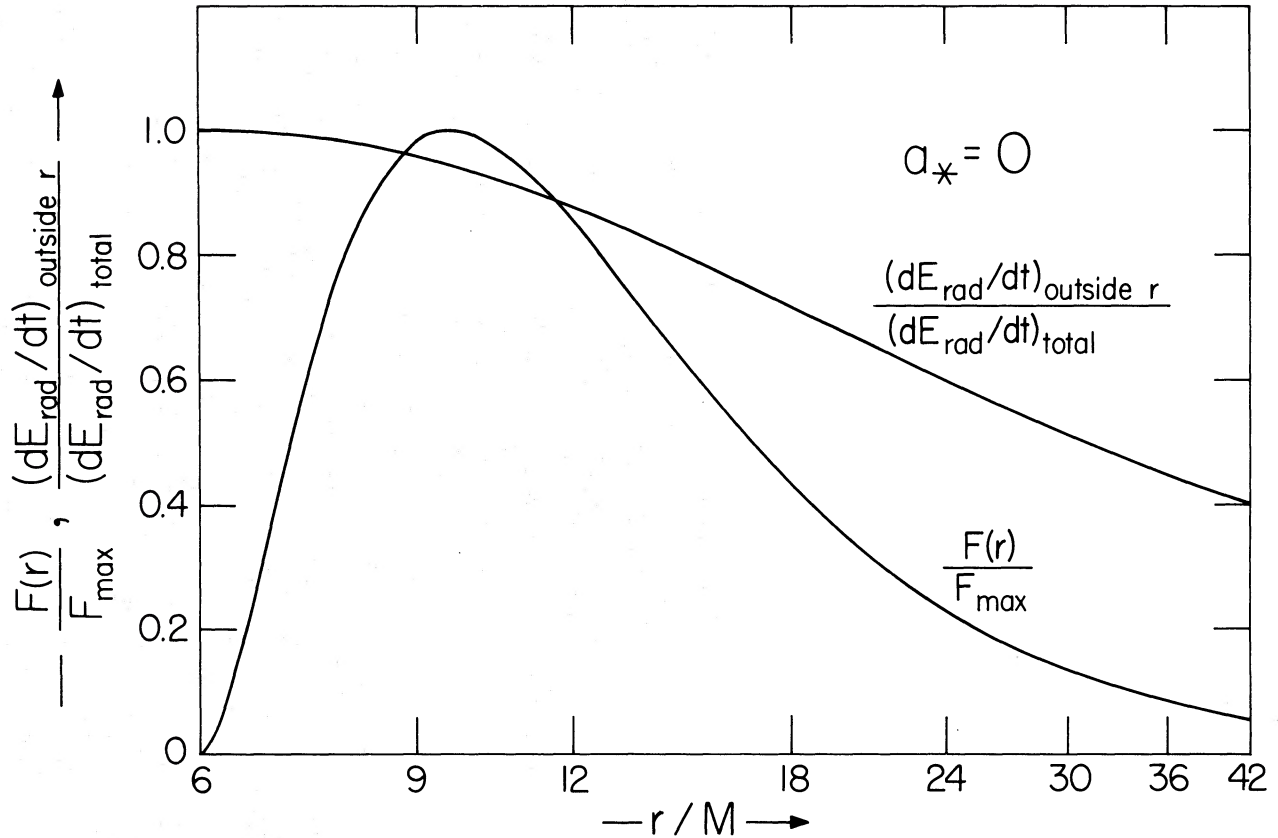


FIG. 4.—The energy radiated (time-average) by a disk around a Schwarzschild black hole. See legend to fig. 3 for explanation of notation. In this case,

$$F_{\max} = 1.37 \times 10^{-5} \dot{M}_0 / M^2.$$

photons of highest energy will come from this region. However, there is not much disk surface area inside the ergosphere, so only 14 percent of all the radiated energy comes from there.

The maximum value of the locally measured flux,  $F_{\max}$ , is far below the value

$$(F_{\max})_{\text{Newton}} = (3/8\pi) [\dot{M}_0 M / (r_{\text{at max}})^3] \quad (8)$$

predicted by elementary Newtonian considerations (eqs. [11b] and [15d, n] of Paper I, with all relativistic corrections dropped, or eq. [5.2.19] of Novikov and Thorne 1973). The values of  $F_{\max}$  given in figures 3 and 4 correspond to

$$\begin{aligned} F_{\max} / (F_{\max})_{\text{Newton}} &= 0.16 & \text{for } a_* = 0.9982, \\ F_{\max} / (F_{\max})_{\text{Newton}} &= 0.10 & \text{for } a_* = 0. \end{aligned} \quad (9)$$

Two effects are responsible for these low maximum fluxes: *First*, in the relativistic regime the gravitational binding energy of an orbit,  $1 - E^+(r)$ , grows less rapidly with decreasing  $r$  than predicted by Newtonian theory; in fact, it “flattens out” into a maximum at the inner edge of the disk ( $r = r_{\text{ms}}$ ) instead of growing as  $M/r$ . Thus, the gravitational energy released by the inflowing matter is less than predicted by Newtonian theory. *Second*, most of the gravitational energy released in the inner, relativistic regions of the disk gets transported out to larger radii by shear stresses before it gets converted into heat and radiated away. This effect is depicted quantitatively in figure 5.

#### IV. SENSITIVITY OF RESULTS TO ASSUMPTIONS

Which of the assumptions made in § II are likely to fail in real astrophysical environments, and how sensitive to such failure are our results on black-hole evolution?

In certain situations three of our assumptions may fail in such a way as to produce very different evolution from that of § III:

i) The accreting matter may not have enough angular momentum to form a disk (specific angular momentum  $\ll$  mass of hole). This is likely to be the case for accretion of interstellar gas onto an isolated hole of normal mass

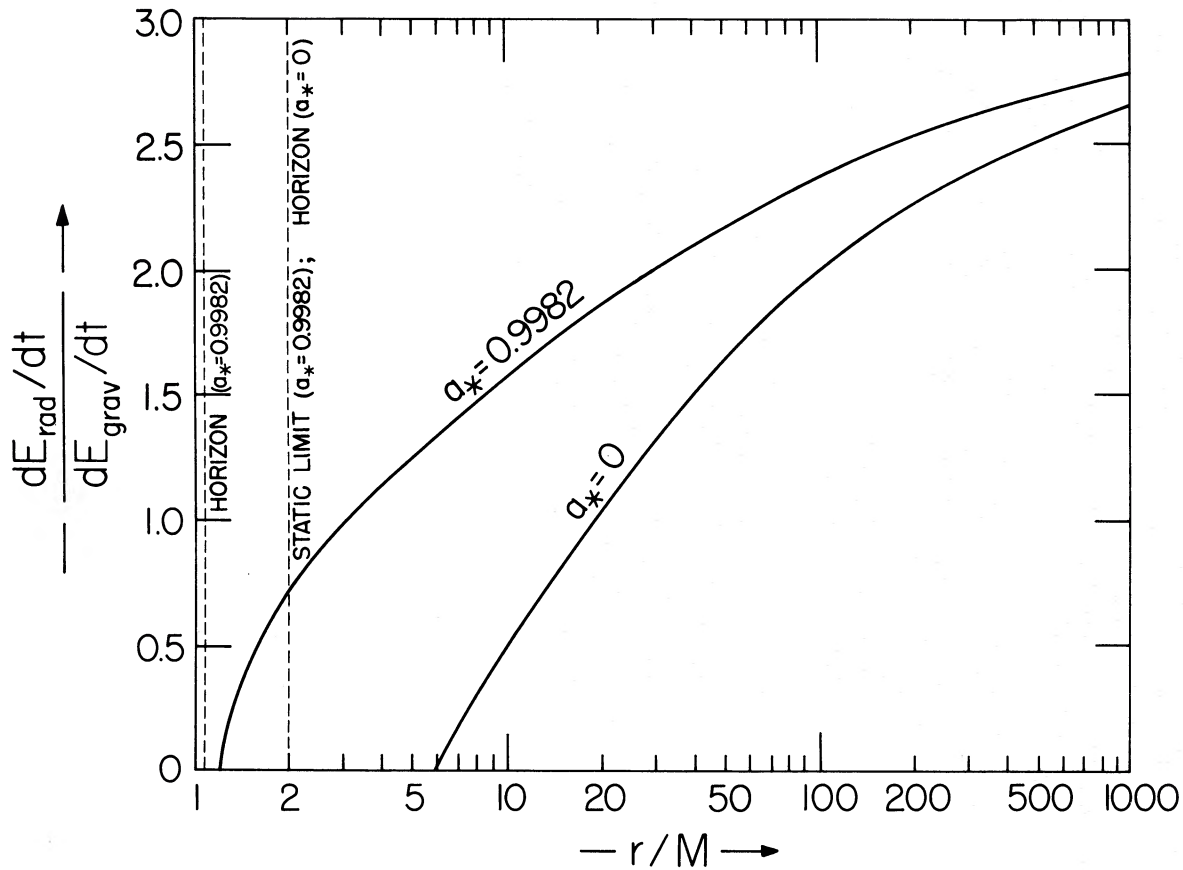


FIG. 5.—The time-averaged rate with which matter at radius  $r$  radiates energy, compared with the rate at which its gravitational binding energy increases (eq. [A6] of Appendix). (How the energy is measured [“energy at infinity” versus “locally measured energy”] and how the rate is measured [“coordinate time” versus “proper time of local, orbiting observer”] are of no consequence here. One need only be careful to measure the gravitational binding energy and rate in the same way as one measures the radiated energy and rate.) In the innermost regions of the disk, far more gravitational energy is being released than is being radiated. The excess energy is transported out to larger radii by shear stresses, and is radiated away there. In the distant, Newtonian region ( $r/M \gg 1000$ ) the matter radiates three times as much energy as local gravity supplies. In essence, the Newtonian region thrives on an energy supply from the relativistic region. For further discussion see Novikov and Thorne (1973, pp. 415–417).

( $\sim 1\text{--}100 M_{\odot}$ ) (p. 407 of Novikov and Thorne 1973). In this case the evolution of the hole will be completely different from that described above. See, e.g., Doroshkevich (1966) or Godfrey (1970).

ii) The plane of the accretion disk at large radii may not coincide with the equatorial plane of the hole. The gravitational fields of the disk and of any companion star, coupling to the hole’s multipole moments, will cause the hole’s spin axis to precess. At the same time, gas and photons being deposited into the hole will change the magnitude of its angular momentum. “Gravitational spin-down” (Press 1972; Hawking and Hartle 1972) presumably will be unimportant. The evolution in this fascinating case will surely differ significantly from that of § III.

iii) The disk may be thick (thickness  $\geq$  radius) in its inner regions, and may even be totally destroyed by (a) radiation pressure due to a supercritical accretion rate (Shakura and Sunyaev 1973), or (b) thermal instabilities due to optical thinness (Pringle and Rees 1972), or (c) a radial secular instability due to “negative mass diffusion coefficient” (Lightman and Eardley 1974; Lightman 1974). In this case, again, the evolution should be considerably different from that of § III.

In these three cases it seems almost certain that the ultimate, limiting value of  $a_*$  will not exceed our value of 0.998—and, hence, that the efficiency for converting rest mass into escaping radiation will not exceed 30 percent.

Other ways in which our assumptions may fail are these:

i) Magnetic fields attached to the disk may reach into the horizon, producing a torque on the hole (Ya. B. Zel’dovich and V. F. Schwartzman, private communication).

ii) The disk will recapture some of the photons it emits, thereby preventing them from going down the hole.

iii) The time-averaged, radial disk structure will be changed by photon recapture and resultant heating, and by magnetic torques that couple the innermost parts of the disk to the hole and couple them to matter that has fallen

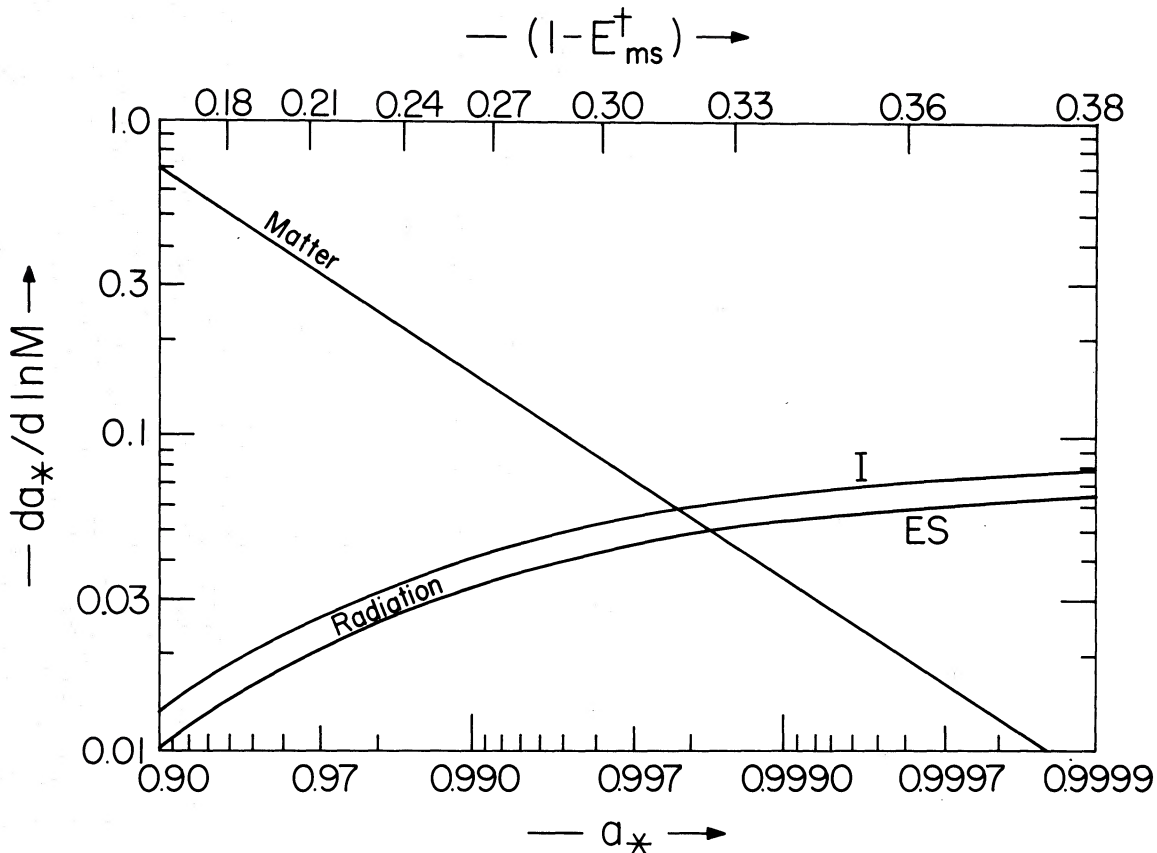


FIG. 6.—The “driving torque” with which matter spins up a black hole, and the counteracting torque of radiation. The curve labeled “Matter” is the value of  $da_*/d \ln M$  (eq. [1a]) when one ignores the effects of radiation. The curves labeled “Radiation” are the negative changes in  $da_*/d \ln M$  due to the inclusion of radiation:

$$-\left(\frac{da_*}{d \ln M}\right)_{\text{radiation}} \equiv -\left[\left(\frac{da_*}{d \ln M}\right)_{\text{total}} - \left(\frac{da_*}{d \ln M}\right)_{\text{matter only}}\right]$$

There are two radiation curves, one for an isotropic emission law (“I”; eq. [5a]); the other for an electron-scattering emission law (“ES”; eq. [5b]). The limiting, canonical black hole occurs at that value of  $a_*$  where the driving torque of matter is counterbalanced by the radiation torque—i.e., where the radiation curve crosses the matter curve. Plotted horizontally are the hole’s value of  $a_*$  (bottom of figure) and the corresponding value of

$$1 - E_{\text{ms}}^+ = \left(\frac{\text{specific binding energy of}}{\text{last stable circular orbit}}\right) = \left(\frac{\text{efficiency for converting rest mass into radiation, ignoring}}{\text{small corrections due to capture of photons by hole}}\right)$$

(top of figure).

out of the disk and is plunging down the hole. The result will be deviations of the emitted photon flux  $F(r)$  from the law derived in Paper I, and deviations of the specific energy and angular momentum of the infalling matter from  $E_{\text{ms}}^+$  and  $L_{\text{ms}}^+$ .

iv) The directionality of the emission,  $I(\theta, \Phi)$ , might be different from the two cases (eqs. [5a, b]) treated here. It seems to me unlikely that these phenomena can affect the evolution of the hole substantially. (For a different opinion, see the end of this section.) To understand my opinion, consider first the directionality of emission [item (iv) above]. We can analyze the effects of directionality by plotting, as functions of  $a_* = a/M$ , the “driving torques” by which matter spins up the hole and radiation retards the spin-up (fig. 6). Notice that the driving torque of matter changes very rapidly with  $a_*$ . As a result, the 20 percent change in the counteracting radiation torque, which occurs when one goes from isotropic emission to electron-scattering emission, produces only a small change in the limiting value of  $a_*$  (change from 0.9978 to 0.9982). The change in  $1 - E_{\text{ms}}^+$  is similarly small (0.318 to 0.324). The steepness of the change of matter torque with  $a_*$  (steepness of matter curve in fig. 6) guarantees that other reasonable emission laws  $I(\theta, \Phi)$  will lead to limiting  $a_*$ ’s near 0.998 and to limiting  $(1 - E_{\text{ms}}^+)$ ’s near 0.32.

Turn now from directionality of emission to all other “perturbing” phenomena taken together—e.g., items (i)–(iii) above. Let the perturbing phenomena produce net changes  $\Delta E^+$  and  $\Delta L^+$  in the energy per unit rest mass

and angular momentum per unit rest mass that go down the hole. Restrict attention to cases, such as (i)–(iii) above, where one can expect

$$\left| \frac{\Delta E^+}{E_{ms}^+} \right| \equiv \left| \frac{\text{energy due to perturbation}}{\text{energy carried by rest mass}} \right| < 0.1, \quad \left| \frac{\Delta L^+}{L_{ms}^+} \right| < 0.1. \quad (10)$$

In such cases, the “counteracting torque” associated with the perturbing phenomena is

$$\begin{aligned} -\left( \frac{da_*}{d \ln M} \right)_{\text{pert}} &= -\left[ \left( \frac{da_*}{d \ln M} \right)_{\text{total}} - \left( \frac{da_*}{d \ln M} \right)_{\text{matter only}} \right] \\ &= -\left[ \frac{1}{M} \frac{(L_{ms}^+ + \Delta L^+)}{(E_{ms}^+ + \Delta E^+)} - \frac{1}{M} \frac{L_{ms}^+}{E_{ms}^+} \right] \simeq \frac{-1}{M} \frac{L_{ms}^+}{E_{ms}^+} \left( \frac{\Delta L^+}{L_{ms}^+} - \frac{\Delta E^+}{E_{ms}^+} \right) \\ &\simeq 2(\Delta E^+/E_{ms}^+ - \Delta L^+/L_{ms}^+) \lesssim 0.1 \quad \text{for } a_* \text{ near } 1. \end{aligned} \quad (11)$$

Since the effects of radiation (“torque”  $\sim 0.05$ ) are always present, we can expect the total “counteracting torque” on the hole to lie in the range  $\sim 0.03$  to  $\sim 0.1$ . By consulting figure 6 we see that the limiting (“canonical”) state of the hole will be

$$0.995 \lesssim a_{*lim} \lesssim 0.999, \quad 0.29 \lesssim (1 - E_{ms}^+)_{lim} \lesssim 0.34. \quad (12)$$

This is not markedly different from the results of § III.

While the above argument seems rather convincing when applied to most perturbing effects, it might fail in the case of magnetic torques [item (iii) above]. In the words of my referee, James M. Bardeen (which echo verbal warnings that I have received from Ya. B. Zel’dovich and V. F. Schwartzman), “It seems quite possible that magnetic stresses could cause large deviations from circular orbits in the very inner part of the accretion disk and change the energy–angular-momentum balance of the accreting matter by an amount of order unity. In this case the limiting value of  $a/M$  may be considerably less than 0.998.”

#### V. RELEVANCE TO ASTROPHYSICAL HOLES

Disk accretion onto black holes is likely to occur in two contexts: (i) for a hole in a close binary system with a normal star, and (ii) for a supermassive hole in the nucleus of a galaxy. (See Novikov and Thorne 1973 for review and references.) In either case the accretion rate can probably not exceed the Eddington limit by more than a factor 3. With a minimum efficiency of 6 percent for converting mass into outgoing radiation, this constraint says

$$0.06 dM/dt \leq L \lesssim 3L_{ED} \simeq (4 \times 10^{38} \text{ ergs s}^{-1})(M/M_{\odot}) \simeq 7 \times 10^{-9} M \text{ yr}^{-1}.$$

Hence, the time scale for substantial evolution of the hole is

$$t_{ev} \equiv M(dM/dt)^{-1} \gtrsim 0.9 \times 10^7 \text{ years}.$$

In binary systems such as Cyg X-1, mass transfer probably cannot last this long, because the *entire* lifetime of a star of  $M > 6 M_{\odot}$  is less than  $6 \times 10^7$  years, and its post-main-sequence lifetime is less than  $2 \times 10^7$  years. Hence, in such systems the hole is not likely to evolve much because of accretion. However, once a supermassive hole forms in the nucleus of a galaxy, it will accrete forever and presumably will evolve substantially (Bardeen 1970).

I thank Stephen W. Hawking for pointing out to me, during the 1972 August Les Houches summer school on black holes, that photons captured by an accreting hole should modify its evolution. That remark was the foundation and motivation for the calculations described in this paper. For other helpful discussions I thank James M. Bardeen and Chris Cunningham. I am grateful to Barbara A. Zimmerman for extensive assistance with the numerical computations. And I thank Douglas M. Eardley, Alan Lightman, and Don Page for helpful comments about the manuscript.

#### APPENDIX

##### DERIVATION OF RESULTS PRESENTED IN §§ III AND IV

We begin with the results shown in figures 3, 4, and 5, since they are independent of the ultimate fates of the photons (capture by hole versus escape to infinity). Our derivation presumes a detailed familiarity with Paper I.

The locally measured flux  $F(r)$ , as shown in figures 3 and 4, was taken directly from equations (I, 11b) and (I, 15d, n). [By (I, 11b) is meant equation (11b) of Paper I.]

The quantity

$$\frac{(dE_{\text{rad}}/dt)_{\text{outside } r}}{(dE_{\text{rad}}/dt)_{\text{total}}}$$

of figures 3 and 4 is derived as follows. Consider the world tube (3-surface) formed by the upper face of the disk outside radius  $r_1$ , as it moves forward in coordinate time by the amount  $\Delta t$ :

$$\mathcal{S}(r_1) = (\text{this 3-surface}) \text{ has } 0 < t < \Delta t, \quad r_1 < r < \infty, \quad z = +H, \quad 0 \leq t \leq \Delta t. \quad (\text{A1})$$

(For the definition of  $\Delta t$ , see assumption [iv] of § II of Paper I.) The flux of “energy-at-infinity” is described by the 4-vector  $\mathbf{E} \equiv -(\partial/\partial t) \cdot \mathbf{T}$ ; hence, the amount of energy-at-infinity that flows across  $\mathcal{S}(r)$  is

$$\begin{aligned} \Delta E &= \int_{\mathcal{S}(r)} -(\partial/\partial t) \cdot \mathbf{T} \cdot d^3\Sigma = \int_{\mathcal{S}(r)} -T_t^z d^3\Sigma_z \\ &= \int_r^\infty \int_0^{\Delta t} \int_0^{2\pi} -u_t q^z (-g)^{1/2} d\varphi dt dr \end{aligned}$$

(see eq. [I, 6a] and the discussion preceding eq. [I, 26])—which reduces to

$$(dE_{\text{rad}}/dt)_{\text{outside } r} \equiv 2\Delta E/\Delta t = 2 \int_r^\infty E^+ F 2\pi r dr. \quad (\text{A2})$$

Here the factor 2 comes from the fact that the lower face radiates as much as the upper face;  $-u_t$  has been replaced by  $E^+$  (eq. [I, 7]);  $(-g)^{1/2}$  has been replaced by  $r$  (eqs. [I, 1e] and [I, 15d]); and equations (I, 2) and (I, 10b) have been used to evaluate the angular and time integrals. The radial integral in (A2) can be evaluated explicitly by invoking equations (I, 15d), (I, 30), (I, 11c), and (I, 15f, i, j). The result is

$$(dE_{\text{rad}}/dt)_{\text{outside } r} = \dot{M}_o (1 - E^+ + \frac{2}{3} r \mathcal{C}^{1/2} f). \quad (\text{A2}')$$

Here  $\mathcal{C}$  and  $f$  are explicit functions of  $r$  given by equations (I, 14) and (I, 15n). The total radiation rate is obtained by evaluating (A2') at the inner edge of the disk,  $r = r_{\text{ms}}$ , and using the boundary condition  $f(r_{\text{ms}}) = 0$  (eq. [I, 34] and preceding discussion). The result is

$$(dE_{\text{rad}}/dt)_{\text{total}} = \dot{M}_o (1 - E^+_{\text{ms}}). \quad (\text{A3})$$

The curves in figures 3 and 4 were constructed using equations (A2') and (A3), together with the explicit forms of the functions  $E^+(r)$ ,  $\mathcal{C}(r)$ , and  $f(r)$  as given in equations (I, 14), (I, 15g, n).

Turn now to the curves in figure 5. Equation (A2) says that the matter in the “ring” between radius  $r$  and radius  $r + \Delta r$  radiates energy-at-infinity at the time-averaged rate

$$dE_{\text{rad}}/dt = (2E^+ F)(2\pi r \Delta r). \quad (\text{A4})$$

When a matter element enters this ring at radius  $r + \Delta r$ , it has specific binding energy of  $1 - E^+(r + \Delta r)$ . Hence, the time-averaged rate at which gravitational binding energy flows into the ring is  $\dot{M}_o [1 - E^+(r + \Delta r)]$ ; and the rate at which it flows out is  $\dot{M}_o [1 - E^+(r)]$ . This means that matter inside the ring is gaining binding energy at the rate

$$dE_{\text{grav}}/dt = \dot{M}_o [1 - E^+(r)] - \dot{M}_o [1 - E^+(r + \Delta r)] = \dot{M}_o E^+_{,r} \Delta r. \quad (\text{A5})$$

Equation (A3) guarantees that the total rate at which energy-at-infinity is radiated (eq. [A4] integrated from  $r_{\text{ms}}$  to  $\infty$ ) equals the total rate at which gravitational binding energy is created (eq. [A5] integrated from  $r_{\text{ms}}$  to  $\infty$ )—i.e., gravitation, and only gravitation, powers the disk. But because stresses transport energy from one region of the disk to another, there is no local equality of  $dE_{\text{rad}}/dt$  and  $dE_{\text{grav}}/dt$ . Figure 5 plots the ratio

$$\frac{dE_{\text{rad}}/dt}{dE_{\text{grav}}/dt} = \frac{(2E^+ F)(2\pi r)}{\dot{M}_o E^+_{,r}} \quad (\text{A6})$$

using  $E^+(r)$  and  $F(r)$  as given in equations (I, 15g), (I, 11b), and (I, 15d, n).

Turn now to the effects of photon capture on the evolution of a black hole (figs. 1, 2, 6; last column of table 1). In the reference frame of an orbiting observer at radius  $r$  (item [xii] of § II) define

$$C(\Theta, \Phi) \equiv \text{“capture function”} = \begin{cases} +1 & \text{if photons emitted into } (\Theta, \Phi) \\ & \text{get captured by hole} \\ 0 & \text{if they escape to infinity.} \end{cases} \quad (\text{A7})$$

Also define the null 4-vector  $n(\Theta, \Phi) \equiv p/p^{(t)}$  ["renormalized photon 4-momentum"] by its components in the observer's orthonormal frame

$$n^{(t)} = 1, \quad n^{(z)} = \cos \Theta, \quad n^{(r)} = \sin \Theta \cos \Phi, \quad n^{(\phi)} = \sin \Theta \sin \Phi. \quad (\text{A8})$$

Use the transformation laws given by Novikov and Thorne (eqs. [5.4.5]) to calculate the components of this renormalized 4-momentum on the coordinate basis

$$-n_t = \mathcal{C}^{-1/2}(\mathcal{G} + x^{-1}\mathcal{D}^{1/2}n^{(\phi)}), \quad n_z = n^{(z)}, \quad (\text{A9a})$$

$$n_\phi = M\mathcal{C}^{-1/2}(x\mathcal{F} + x^2\mathcal{B}\mathcal{D}^{1/2}n^{(\phi)}), \quad n_r = \mathcal{D}^{-1/2}n^{(r)}. \quad (\text{A9b})$$

The constants of the motion for the geodesic orbit of a photon emitted in the  $\Theta, \Phi$  direction from radius  $r$  are

$$\begin{aligned} j &\equiv a_*^2 - a_*(L_z/ME) = a_*^2 - a_*n_\phi/(-Mn_t) \\ &= a_*^2 - a_* \frac{x\mathcal{F} + x^2\mathcal{B}\mathcal{D}^{1/2} \sin \Theta \sin \Phi}{\mathcal{G} + x^{-1}\mathcal{D}^{1/2} \sin \Theta \sin \Phi}, \end{aligned} \quad (\text{A10a})$$

$$\begin{aligned} k &\equiv \mathcal{K}/(ME)^2 = (j/a_*)^2 + (rn_z)^2/(-n_tM)^2 \\ &= \left(\frac{j}{a_*}\right)^2 + \frac{x^4\mathcal{C} \cos^2 \Theta}{(\mathcal{G} + x^{-1}\mathcal{D}^{1/2} \sin \Theta \sin \Phi)^2} \end{aligned} \quad (\text{A10b})$$

Here  $L_z$ ,  $E$ , and  $\mathcal{K}$  are the standard Carter (1968) constants of the motion in the notation of Misner, Thorne, and Wheeler ("MTW") (1973; § 33.5); and we have evaluated them at the point (radius  $r$ , polar angle  $\theta = \pi/2$ ) where the photons are emitted, using the relation  $p_\theta/p_t = (rn_z)/n_t$ . Whether a photon gets captured by the hole or escapes to infinity can be determined by examining its radial equation of motion (MTW, eq. [33.32b]). Rearranged and converted to our notation, that equation becomes

$$W(r, \theta)(dr/d\lambda)^2 + V(r) = 1/k, \quad (\text{A11})$$

where

$$W(r, \theta) = k^{-1}E^{-2}(r^2 + a^2 \cos^2 \theta)^2(r^2 + M^2j)^{-2}, \quad (\text{A12a})$$

$$V(r) = M^2(r^2 - 2Mr + a^2)(r^2 + M^2j)^{-2}. \quad (\text{A12b})$$

(Note that  $k = \mathcal{K}/(ME)^2$  is positive for all photons emitted from the disk; cf. p. 899 of MTW.)  $V(r)$  plays the role of an effective potential, and  $1/k$  is an effective energy for the photon motion. One can show that in the region outside the hole [ $r > r_+ = M + (M^2 - a^2)^{1/2}$ ], and for any (fixed) value of  $j$ ,  $V(r)$  has precisely one extremum. Moreover, that extremum is always a maximum. It is located at radius

$$r_m = M(-j)^{1/2} \quad \text{if } j \leq -(r_+/M)^2 \quad [\text{in this case } V(r_m) = +\infty], \quad (\text{A13a})$$

$$r_m = R_m(j, a_*) \quad \text{if } j > -(r_+/M)^2 \quad [\text{in this case } V(r_m) \text{ is finite}]. \quad (\text{A13b})$$

Here  $R_m(j, a_*)$  is the function

$$R_m = M\{1 + [\beta + (\beta^2 - \alpha^3)^{1/2}]^{1/3} + \alpha[\beta + (\beta^2 - \alpha^3)^{1/2}]^{-1/3}\} \quad \text{if } \beta^2 \geq \alpha^3; \quad (\text{A14a})$$

$$R_m = M\{1 + 2\alpha^{1/2} \cos [\frac{1}{3} \cos^{-1}(\beta/\alpha^{3/2})]\} \quad \text{if } \beta^2 \leq \alpha^3; \quad (\text{A14b})$$

$$\alpha \equiv 1 + \frac{1}{3}(j - 2a_*^2), \quad \beta \equiv 1 - a_*^2. \quad (\text{A14c})$$

From the above properties of the effective potential, and from the equation of motion (A11), one can easily deduce the following algorithm for computing the capture function  $C(\Theta, \Phi)$ :

- i) Specify  $\Theta$  and  $\Phi$ , and set  $C = 1$ .
- ii) If [ $j < -(r_+/M)^2$ ] & [ $(r/M) \leq (-j)^{1/2}$ ], then terminate.
- iii) If [ $j < -(r_+/M)^2$ ] & [ $(r/M) > (-j)^{1/2}$ ], then set  $C = 0$  and terminate.
- iv) Calculate  $R_m$  using equations (A14), and calculate  $V(R_m)$  using equation (A12b).
- v) If [ $r < R_m$ ] & [ $\cos \Phi > 0$ ] & [ $1/k > V(R_m)$ ], then set  $C = 0$  and terminate. (A15)
- vi) If [ $r > R_m$ ] & [ $\cos \Phi > 0$ ], then set  $C = 0$  and terminate.
- vii) If [ $r > R_m$ ] & [ $\cos \Phi < 0$ ] & [ $1/k < V(R_m)$ ], then set  $C = 0$  and terminate.
- viii) Terminate.

This algorithm was used in the computations reported in this paper. For an alternative method of calculating capture versus escape, see pp. 231–233 of Bardeen (1973).

In calculating the evolution of the hole we shall need an expression for the time-averaged stress-energy tensor  $\langle T \rangle$  of all photons immediately above the surface of the disk—and that  $\langle T_{\text{DH}} \rangle$  of those photons that will eventually go down the hole. We write  $\langle T \rangle$  and  $\langle T_{\text{DH}} \rangle$  as integrals over photon momentum space:

$$\langle T^{(\alpha)(\beta)} \rangle = \int \langle \mathcal{N} \rangle p^{(\alpha)} p^{(\beta)} d^3 p / p^{(t)}, \quad \langle T_{\text{DH}}^{(\alpha)(\beta)} \rangle = \int C \langle \mathcal{N} \rangle p^{(\alpha)} p^{(\beta)} d^3 p / p^{(t)}. \quad (\text{A16})$$

(Exercise 22.18 of MTW.) The number density in phase space  $\mathcal{N}$  is related to the locally measured specific intensity  $I_\nu$  and locally measured frequency  $\nu = p^{(t)}/h$  by

$$\mathcal{N} = h^{-4} (I_\nu / \nu^3),$$

where  $h$  is Planck's constant (MTW, eq. [22.49]). Hence, the time-averaged intensity  $\langle I \rangle$  is given by

$$\langle I \rangle \equiv \int \langle I_\nu \rangle d\nu = \int \langle \mathcal{N} \rangle (p^{(t)})^3 dp^{(t)}.$$

We shall embody the directionality of  $\langle I \rangle$  in a function  $S(\Theta, \Phi)$  normalized such that

$$\int_0^{\pi/2} \int_0^{2\pi} S(\Theta, \Phi) \cos \Theta \sin \Theta d\Phi d\Theta = 1. \quad (\text{A17})$$

Thus,

$$S = 1/\pi \quad \text{for isotropic emission (eq. [5a]),} \quad (\text{A18a})$$

$$S = (3/7\pi)(1 + 2 \cos \Theta) \quad \text{for electron scattering atmosphere (eq. [5b]).} \quad (\text{A18b})$$

In terms of  $S$  we write

$$\langle I \rangle = \int \langle \mathcal{N} \rangle (p^{(t)})^3 dp^{(t)} = I_0 S(\Theta, \Phi). \quad (\text{A19})$$

We must choose the normalization factor  $I_0$  such that  $\langle \mathcal{N} \rangle$  gives the correct total emitted flux:

$$\begin{aligned} F(r) &= [\text{Expression (I, 11b)}] = \langle T^{(t)(z)} \rangle = \int \langle \mathcal{N} \rangle (p^{(t)})^2 n^{(z)} d^3 p / p^{(t)} \\ &= \int_0^{\pi/2} \int_0^{2\pi} \left[ \int_0^\infty \langle \mathcal{N} \rangle (p^{(t)})^3 dp^{(t)} \right] \cos \Theta \sin \Theta d\Phi d\Theta \\ &= I_0 \int_0^{\pi/2} \int_0^{2\pi} S \cos \Theta \sin \Theta d\Phi d\Theta = I_0. \end{aligned}$$

[Here we have used the relations

$$\mathbf{p} = p^{(t)} \mathbf{n}, \quad n^{(z)} = \cos \Theta, \quad d^3 p = (p^{(t)})^2 dp^{(t)} \sin \Theta d\Theta d\Phi,$$

as well as eqs. (A16), (A17), and (A19).] Thus, we must set

$$I_0 = F(r). \quad (\text{A20})$$

We are now ready to calculate the time-averaged rates at which photons carry energy and angular momentum down the hole, and thereby increase the hole's mass and angular momentum. These rates, expressed as integrals over the surface of the entire disk [ $\mathcal{S}(r_{\text{ms}})$ ; eq. (A1)] are

$$\begin{aligned} (dM/dt)_{\text{radiation}} &= (1/\Delta t) 2 \int_{\mathcal{S}(r_{\text{ms}})} (-\partial/\partial t) \cdot \mathbf{T}_{\text{DH}} \cdot d^3 \Sigma \\ &= (1/\Delta t) 2 \int \int \int (-T_t^z)_{\text{DH}} (-g)^{1/2} d\varphi dt dr = 2 \int \langle (-T_t^z)_{\text{DH}} \rangle 2\pi r dr \\ &= 2 \int \int \int \int [C \langle \mathcal{N} \rangle (-n_t) n^z (p^{(t)})^2] [p^{(t)} dp^{(t)} \sin \Theta d\Phi d\Theta] 2\pi r dr \\ &= \int_{r_{\text{ms}}}^\infty \left[ \int_0^{\pi/2} \int_0^{2\pi} C S (-n_t) \cos \Theta \sin \Theta d\Phi d\Theta \right] 2F 2\pi r dr; \quad (\text{A21}) \end{aligned}$$

and similarly,

$$(dJ/dt)_{\text{radiation}} = \int_{r_{\text{ms}}}^{\infty} \left[ \int_0^{\pi/2} \int_0^{\pi} CSn_{\theta} \cos \Theta \sin \Theta d\Phi d\Theta \right] 2F2\pi r dr. \quad (\text{A22})$$

In equation (A21): (i) the second expression is analogous to that used in deriving equation (A2); (ii) the factor 2 in the second expression accounts for the two faces of the disk; (iii) the fourth expression uses the time-averaging procedure of Paper I; (iv) the fifth expression uses the relation  $p = p^{(i)}\mathbf{n}$  as well as equation (A16); (v) the sixth expression uses equations (A19) and (A20), and the relation  $n^z = n^{(z)} = \cos \Theta$ .

When evaluating the integrals in (A21) and (A22) one uses equations (I, 11b) and (I, 15d, n) for  $F(r)$ ; algorithm (A15) for  $C(\Theta, \Phi)$ ; any desired directionality function  $S(\Theta, \Phi)$ —subject only to the normalization condition (A17); and expressions (A8) and (A9) for  $-n_r(r, \Theta, \Phi)$  and  $n_{\theta}(r, \Theta, \Phi)$ .

In calculating the evolution of the hole one must include, in addition to the radiation effects (eqs. [A21] and [A22]), also the effects of the matter falling down the hole:

$$(dM/dt)_{\text{matter}} = \dot{M}_o E^{\dagger}_{\text{ms}}, \quad (dJ/dt)_{\text{matter}} = \dot{M}_o L^{\dagger}_{\text{ms}}. \quad (\text{A23})$$

Hence, the equations for the evolution are

$$\begin{aligned} dM/dt &= \dot{M}_o E^{\dagger}_{\text{ms}} + (dM/dt)_{\text{radiation}}, \\ dJ/dt &= \dot{M}_o L^{\dagger}_{\text{ms}} + (dJ/dt)_{\text{radiation}} \end{aligned} \quad (\text{A24})$$

—or, equivalently,

$$\frac{da_*}{d \ln M} = \frac{d(J/M^2)}{d \ln M} = \frac{1}{M} \frac{L^{\dagger}_{\text{ms}} + \dot{M}_o^{-1}(dJ/dt)_{\text{radiation}}}{E^{\dagger}_{\text{ms}} + \dot{M}_o^{-1}(dM/dt)_{\text{radiation}}} - 2a_*, \quad (\text{A25a})$$

$$\frac{dM}{dM_o} = E^{\dagger}_{\text{ms}} + \dot{M}_o^{-1}(dM/dt)_{\text{radiation}}. \quad (\text{A25b})$$

The evolution shown in figures 1 and 2 was derived by numerical integration of equations (A21) and (A22) followed by numerical solution of the differential equations (A25a, b). The curves in figure 6 were evaluated using equation (A25a) plus the numerical integrations of (A21) and (A22). The efficiencies in the last column of table 1 are

$$\text{Efficiency} = \dot{M}_o^{-1}(\dot{M}_o - dM/dt) = 1 - E^{\dagger}_{\text{ms}} - \dot{M}_o^{-1}(dM/dt)_{\text{radiation}}. \quad (\text{A26})$$

#### REFERENCES

- Bardeen, J. M. 1970, *Nature*, **226**, 64.  
 ———. 1973, in *Black Holes*, ed. C. DeWitt and B. DeWitt (New York: Gordon & Breach).  
 Bardeen, J. M., Carter, B., and Hawking, S. W. 1973, *Comm. Math. Phys.*, **31**, 161.  
 Carter, B. 1968, *Phys. Rev.*, **174**, 1559.  
 Chandrasekhar, S. 1950, *Radiative Transfer* (Oxford: Oxford University Press).  
 Doroshkevich, A. G. 1966, *Astr. Zhur.*, **43**, 105; terrible English transl. in *Soviet Astr.—AJ*, **10**, 83.  
 Godfrey, B. 1970, *Phys. Rev.*, **D1**, 2721.  
 Hawking, S. W., and Hartle, J. B. 1972, *Comm. Math. Phys.*, **27**, 283.  
 Lightman, A. P. 1974, paper submitted to *Ap. J.*  
 Lightman, A. P., and Eardley, D. 1974, *Ap. J. (Letters)*, **187**, L1; also available as Caltech Orange Aid Preprint No. 340.  
 Lynden-Bell, D. 1969, *Nature*, **223**, 690.  
 Misner, C. W., Thorne, K. S., and Wheeler, J. A. 1973, *Gravitation* (San Francisco: Freeman); (cited in text as "MTW").  
 Novikov, I. D., and Thorne, K. S. 1973, in *Black Holes*, ed. C. DeWitt and B. DeWitt (New York: Gordon & Breach).  
 Page, D. N., and Thorne, K. S. 1974, *Ap. J.*, **191**, 499 (preceding paper; cited in text as Paper I).  
 Press, W. H. 1972, *Ap. J.*, **175**, 243.  
 Pringle, J. E., and Rees, M. J. 1972, *Astr. and Ap.*, **21**, 1.  
 Shakura, N. I., and Sunyaev, R. A. 1973, *Astr. and Ap.*, **24**, 337.

KIP S. THORNE

Kellogg Radiation Laboratory, 106-38, California Institute of Technology, Pasadena, California 91109

